Volume 9, Issue 5, 2019, 4272 - 4278 ISSN 2069-5837

Biointerface Research in Applied Chemistry

www.BiointerfaceResearch.com

https://doi.org/10.33263/BRIAC95.272278

Original Research Article Open Access Journal

Received: 30.07.2019 / Revised: 05.09.2019 / Accepted: 12.09.2019 / Published on-line: 15.09.2019

Novel flame retardant and antibacterial agent containing MgO NPs, phosphorus, nitrogen and silicon units for functionalise cotton fabrics

Ahmed G. Hassabo [1,*], Amina L. Mohamed [1]

[1]National Research Centre (NRC) (Scopus affiliation ID 60014618), Textile Industries Research Division (TIRD), Pre-treatment and Finishing of Cellulose based Textile Department (PFCTD), 33-El-Behouth St. (former El-Tahrir str.), Dokki, P.O. 12622, Giza, Egypt

*corresponding author e-mail address: ***aga.hassabo@hotmail.com***

ABSTRACT

During this research, Magnesium oxide (MgO) nanoparticles were synthesised synthesized using Licorice root extract. Synthesized nanoparticles have been characterized using FT-IR, TEM and XRD. The analysis confirmed that the nanoparticles size were ranged from 20 to 40 nm with cubic structure. This nanoparticle was used in the formulation with new synthesised composite containing phosphor, nitrogen and silicon to enhance thermal and flame retardant properties of cotton fabrics. This composite has synthesised via reaction of 3-(hydroxy(phenyl)phosphoryl)propanoic acid and Triethanolamine, and then with triethoxy(3-isocyanatopropyl)silane. Prepared composite was confirmed through NMR and FT-IR measurements. Treated fabric with prepared composite and nanoparticles have been evaluated through elemental analysis, TGA, LOI, antibacterial, mechanical and physical properties. The nanoparticle coated fabrics with prepared composite showed a good degree of microbial resistance and excellent fire proofing rating

Keywords: *MgO nanoparticles; composite containing Si/P/N, flame retardant and cotton fabrics.*

1. INTRODUCTION

Flame retardant textiles was an important functional finish to fulfill flammability standards for textiles. Major flame-retardants materials are synthetic compounds utilized in textiles, thermoplastics, thermosets and coatings that resist the fire spreading [1].

In numerous regards the ignition of polymers is like the burning of numerous other solid materials; nevertheless, the inclination of polymers to spread fire far from a flame source is basic in light of the fact that numerous polymers were melt. Along these lines, it is constantly critical to test the instability of polymeric materials under conditions near those of the last applications or even in get together with different materials. For instance, fire spread can be estimated in both positions (vertical and horizontal) [2, 3].

Flame retardant compounds containing halogen have played and keep on having a huge influence in flame retardancy. In any case, for the most part in light of ecological and environmental concern, there was developing for non-halogenated flame retardant materials. The extensive number of research is concern around non-halogenated fire retardants compounds; for example; antimony trioxide, [1] phosphorus-containing materials, [4] fumed silica, [5] iron, [6] metal oxides, [7] nickel phosphates, [8] and montmorillonite [9, 10].

Thermal decomposition of cellulose-containing fabrics changing using chemical containing phosphorus. These chemicals are important as flame retardant compounds because they increasing the residual char and decreasing the pyrolysis temperature. Phosphorus containing materials are working as acid precursors through burning or pyrolysis, and the produced acids is a reason for decomposition of the carbohydrates [11].

Licorice is Glycyrrhiza Glabra root's of containing numerous compounds. Extracted Licorice containing healing materials, flavonoids and different estrogens from plant (phytoestrogens). Without a doubt, licorice has sweetness compounds from glycyrrhizin (sweeter than sugar). The chemical structure of glycyrrhizin shown in Figure 1 [12-16].

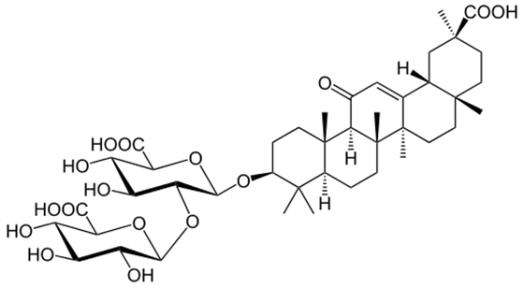

Figure 1. Chemical structure of glycyrrhizin from Licorice.

Magnesium oxide nanoparticles (MgO-NPs) have an excellent structural characteristic, which provides an exceptional physical and chemical properties [17, 18]. MgO nanoparticles have synthesised through several methods [17, 19]. Wet chemical procedure used to synthesis MgO nanoparticles are affected both size and surface morphology of particles which depends on many factors for example, temperature, hydrolysis rate of magnesium salts, base type, salt concentration, drying and calcination temperature [20-22].

During this research, MgO nanoparticles have been synthesised using Licorice root extract, after that, it was used in the formulation with new synthesised composite containing phosphor, nitrogen and silicon to improve the flame retardant properties of cellulose containing fabrics [23].

2. MATERIALS AND METHODS

2.1. Materials.

Cotton fabric (185 g/m^2) was used and supplied by Ghazel El-Mahala for Textile Industry Co., Egypt. Cotton fibre was washed with 5% of sodium lauryl sulphate (SLS) for 30 min at 40°C, then rinsing with distilled water and dried at 100°C for 5 min.

3-(hydroxy(phenyl)phosphoryl)propanoic acid (HPPPA) was purchased from I-TAI Chemicals Inc. Triethanolamine (TEA), triethoxy(3-isocyanatopropyl)silane (TIS), N,N-dimethylacetamide (DMAc), N,N'-dicyclohexylcarbodiimide (DCC), tetrahydrofuran (THF) and trifluoroacetic acid (TFA) were purchased from Sigma-Aldrich.

Two bacterial strains from the Faculty of Agriculture, Cairo University, Egypt were used *(Escherichia coli (E. coli)* as Gram-negative bacteria (G-ve) and *Staphylococcus aureus (S. aureus*) as Gram-positive bacteria (G+ve)). Both strains were selected because they are the most frequent bacteria in the cellulose infection.

2.2. Synthesis.

2.2.1. Extraction methods of Licorice root (LRE). Licorice root extract (LRE) was prepared according to modified method from Mohamed et. al. [24] using water for extraction as follow: 50 g plant was mixed with 500 ml water in a round flask and kept under reflux at boiling temperature for 4 h, then cooled down and filtered. The extract was kept in 4°C.

2.2.2. Synthesis of MgO nanoparticles using Licorice root extract. Synthesized MgO nanoparticles (MgO-NPs) were occurred using sol-gel method [25] as follow: 10 g magnesium nitrate hexahydrate ($Mg(NO_3)_2.6H_2O$) was added to Licorice root extract, under stirring at room temperature for 4 h and pH 9 (adjusted with 0.2 M aqueous NaOH solution). After that, magnesium hydroxide ($Mg(OH)_2$) was precipitated as a brown colloidal particles at the bottom of the flask. Precipitated particles were collected after one day by centrifugation at 12000 rpm for 20 min, then dried in oven at 110°C. Calcination process was carried out in furnace at 450°C for 3 h then MgO nanoparticles (MgO-NPs) were obtained.

2.2.3. Synthesis of HAPPA. First, in 500 ml round flask HPPPA (2.14 g, 0.01 mole) was dissolved in 100 ml of THF. After that, TEA (1.49 g, 0.01 mole; 1: 1 mole ratio of HPPPA/TEA) and DCC were added and dissolved in the solution. After completely dissolving, two drops of TFA were added as a catalyst and the temperature was raised to 65°C under stirring (300 rpm) for 12 h at this temperature. Then, the HAPPA was obtained using rotary evaporator, and then dried at 50°C for 1 d (see Scheme 1).

2.2.4. Synthesis of PNSi composite. In 500 ml round flask HAPPA (3.45 g, 0.01 mole) and TIS (5 g, 0.02 mole; 1: 2 mole ratio of HAPPA: TIS) were mixed with 100 ml of DMAc at 80°C and the reaction was kept under stirring (300 rpm) for 8 h at this temperature. Then, the PNSi composite was obtained using rotary evaporator, and then dried at 50°C for 1 d (see Scheme 1).

2.2.5. Fabric Treatment. Bleached cellulose fabrics were performed treated using padding-drying-curing finishing procedure. Prepared composite (PNSi, 0, 10, 30 and 50 g/l) in presence or absence of prepared MgONPs (10 g/l) were suspended in water under stirring for 15 min. Butanetetreacarboxylic acid (BTCA; 10 g/l) and sodium hypophosphite (SHP; 5 g/l) were added gradually and stirred for another 15 min. Then cellulosic fabrics were immersed in the solution for 5 min and padded with 80 % wet pickup, dried at 100°C for 5 min and cured at 130°C for 3 min.

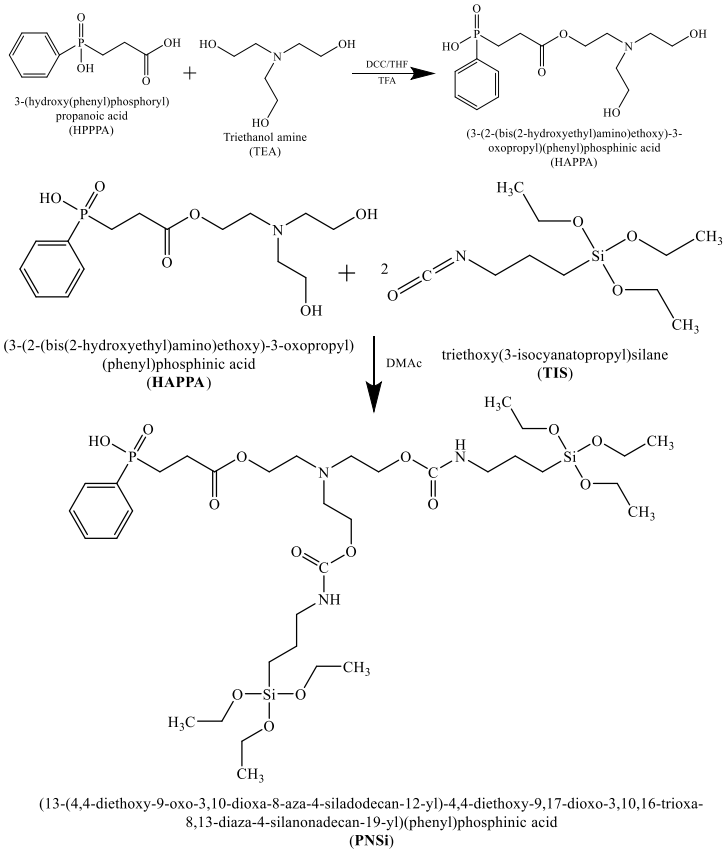

Scheme 1. Schematic reaction for synthesis of HAPPA and PNSi

2.3. Characterization.

2.3.1. Characterisation of MgO Nanoparticles. The structural Characterisation of the synthesised MgO-NPs was provided by Transmission Electron Microscopy (JEOLJEM 2100). Dynamic Light Scattering (DLS) technique was used to calculate the average particles size of the nanoparticles. X-ray Diffraction (XRD) technique was used to investigate the phase and structural behaviour of MgO-NPs using CuK at 1.514Å with nickel as filter and scanning range as 0.2°/min at 20-80°C. In addition, the antibacterial activity of MgO-NPs has been evaluated using disc diffusion method [26].

2.3.2. Characterisation of HAPPA and PNSi composite. Characterisation of HAPPA and PNSi were occurred by measuring the FT-IR which confirmed produced both material HAPPA and PNSi. Fourier Transform Infrared (FT-IR) spectroscopy (Shimadzu FT-IR-8400 S, Japan) was used to identify the presence of new function groups in the prepared materials. ^{1}H NMR (in DMSO-d_6) spectra of the prepared materials were measured using a Bruker Avance 300 spectrometer (300MHz).

2.3.3. Characterisation of the treated fabrics. Thermal behaviour of treated fabrics were investigated using a thermal gravimetrical analyser Mettler-Toledo DTA/TGA instrument where the temperature ranges from 25 to 700°C, The samples were heated at the rate of 10°C/min from room temperature to 700°C under nitrogen flow [27]. Limiting oxygen index (LOI) values of some samples were measured according to ASTM standard method D2863-08. [28] Fire resistance behaviour of treated fabrics was evaluated using vertical test method in fire resistance of treated fabrics[29]. Tensile strength and elongation at break are carried out according to the ASTM Standard Test Method D1683/D1683M [30] on a tensile strength apparatus type FMCW 500 (Veb Thuringer Industrie Werk Rauenstein 11/2612 Germany) at 25°C and 65% relative humidity. The results quoted are the mean of 5 breaks for the warp direction with test length of 20 cm at a constant breaking time of 20 seconds, load scale 10–50 Kg. Stiffness was determined according to ASTM Test Method D 1388-14e1 [31] using the cantilever apparatus. Surface roughness was monitored according to JIS 94 standard, using surface roughness measuring instrument, SE 1700, made in Japan.

Disc diffusion method [26] was used to investigate the antimicrobial activity of treated fabrics. 10 mm diameter from the untreated and treated fabrics were cut using suitable cutter. A microbial culture impeded in nutrient agar and then incubated. Prepared fabric was then gently placed with the help of a forceps on top of the agar plate containing the test organism. The plate was incubated at 30°C for 72 h. Inhibition one distance from disc circumference in mm) was determined and recorded for each sample. All data consisted of the means of at least three parallel experiments. Laundering of treated fabrics was performed using non-ionic wetting agent 0.5 g/l for 45 min followed by drying at 70°C for each laundering.

3. RESULTS

3.1. Characterisation of MgO nanoparticles (MgO-NPs). X-Ray diffraction pattern for synthesized MgONPs in the 2θ range from 20 to 80° at λ = 1.5418 Å at 0.4°/min scan speed to confirm the structure shown in Figure 2. X-Ray spectrum provides a good crystallinity for MgONPs as a result of presence a four characteristic peaks at 36.11, 43.23, 62.13 and 75.62° which indicating the crystalline nature of MgO-NPs with face-centred cubic structure (fcc) of MgO [32].

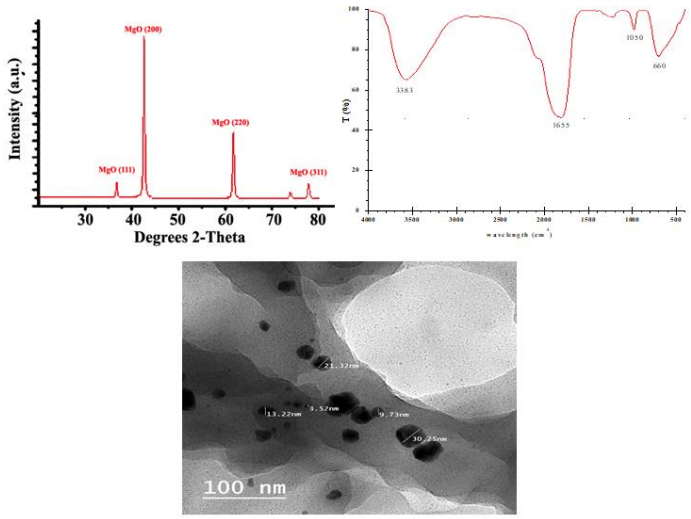

Figure 2. XRD pattern, FT-IR spectroscopy sand TEM image for MgO-NPs.

In addition, there are no characteristics peaks detected for $Mg(OH)_2$ or any other impurities. Furthermore, the average size of synthesised MgO-NPs was obtaining using Debye -Scherrer's equation [26]:

$$d = 0.9 \lambda / \beta \cos \theta$$

where d is the crystallite size in nm, λ is the X-ray wavelength, β is the full width at half maximum (FWHM) of the diffraction peak, and θ is the diffraction angle of the diffraction peaks. Therefore, average particle sizes for MgO-NPs were 16 nm.

FT-IR spectra for MgO-NPs which shown in Figure 2 provide a sharp peak ascribed to antisymmetric stretching vibration of OH groups in the crystal structure of $Mg(OH)_2$ because of presence of water at 3383 cm^{-1}. Another peak was observed at 660 cm^{-1} assigned to Mg-O stretching vibration bond [33] at 1050 cm-1 thee is an absorption peak corresponds to the bending vibration of Mg–OH stretching. Another peak at 1655 cm-1 was presented as a result of the stretching vibration of water [34].

From TEM pictures presented in the Figure 2, the MgO-NPs sizes were in the range of 11-20 nm and hygroscopic in nature, which is similar to the calculated value from XRD.

3.2. Characterisation of HAPPA and PNSi composite.

Characterisation of HAPPA and PNSi were occurred by measuring their FT-IR which confirmed produced both materials; HAPPA and PNSi. FT-IR spectrum of HAPPA is shown in Figure 3. Spectra of HAPPA provide a peak at 3377 cm^{-1} which corresponding to a hydroxyl group. Two peaks at 2943 and 2876 cm^{-1} for symmetrical and asymmetrical stretching vibration of CH_2 were also presented. These peaks were attributed to the reaction with TEA. Furthermore, the presence of peak at 1723 cm^{-1} (carbonyl group; C = O) is an indication for synthesis of HAPPA. The resonance absorption peak of the C = C in benzene ring appeared at 1590 cm^{-1}, also the C-O stretching vibration peak at 1216 cm^{-1}. The two peaks at 1180 and 1435 cm^{-1} are corresponding to P = O and P-Ph respectively[35].

The FT-IR spectra of PNSi in Figure 3 have some important peaks, at 3325 cm^{-1} corresponding to the –NH stretching vibration peak, at 2945 and 2869 cm^{-1} are the stretching vibrations of CH_2, and the peak at 1725 cm^{-1} represents carbonyl group (C=O). The peaks at 1633 and 1581 cm^{-1} are due to the C=C stretching vibration. The C-O stretching vibration peak appears at 1213 cm^{-1}. In addition, there is no peak observed corresponding to the free NCO group at 2230–2273 cm^{-1}. Therefore, the TSI was fully reacted with HAPPA. Specifically, the band lay between 950-1250 cm^{-1} was assumed to the presence of asymmetric stretching vibrations bands from the Si-O bonds[36]. In addition, a specific peak corresponding to Si-C was observed at 1275 cm^{-1}.

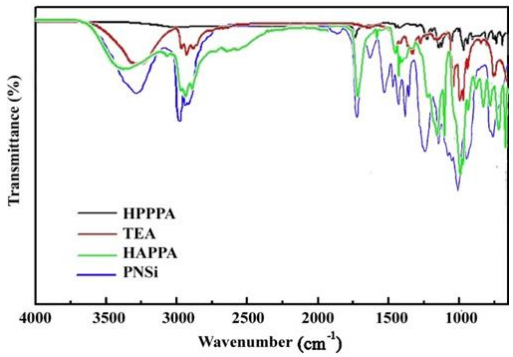

Figure 3. FT-IR spectra of the HPPPA, TEA, HAPPA and PNSi.

Characterisation of HAPPA and PNSi were occurred by measuring the ^{1}H-NMR which confirmed the produced material PNSi. δ ppm of ^{1}H-NMR were listed below.

^{1}H-NMR of HAPPA (chemical formula: $C_{15}H_{24}NO_6P$, Mwt: 345.33 g/mole, elemental analysis: C, 50.3 %; H, 8.2 %; N, 5.5 %; O, 26.1 %; P, 3.4 %; Si, 6.5 %) in DMSO-d6 were presented in Figure 4. δ ppm: a and e: 7.32 (m, 2H, aromatic), b and d: 7.68 (m, 2H, aromatic), c: 7.51 (m, 2H, aromatic), g: 4.92 (s, 1H, OH), h and m: 2.92 (m, 2H, CH_2), i: 2.76 (m, 2H, CH_2), l: 4.31 (m, 2H, CH_2), o and r: 2.51 (m, 2H, CH_2), p and s: 3.38 (m, 2H, CH_2) and q and t: 4.12 (s, 1H, OH)

^{1}H-NMR of PNSi (chemical formula: $C_{35}H_{66}N_3O_{14}PSi_2$, Mwt.: 840.06 g/mole, elemental analysis: C, 52.1 %; H, 7.2 %; N, 4.1 %; O, 27.9 %; P, 8.7 %) in DMSO-d6 were presented in Figure 4. δ ppm: a and e: 7.26 (m, 2H, aromatic), b and d: 7.38 (m, 2H, aromatic), c: 7.31 (m, 2H, aromatic), g: 4.82 (s, 1H, OH), h: 3.02 (m, 2H, CH_2), i: 2.82 (m, 2H, CH_2), l and p: 4.38 (m, 2H, CH_2), m and o: 2.98 (m, 2H, CH_2), s: 6.83 (s, 1H, NH), t: 3.22 (m, 2H, CH_2), u: 1.62 (m, 2H, CH_2), v: 0.71 (m, 2H, CH_2), y: 3.91 (m, 2H, CH_2) and z: 1.24 (t, 3H, CH_3)

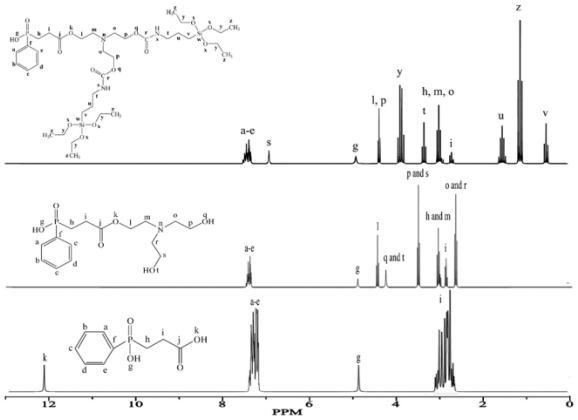

Figure 4. ^{1}H-NMR spectra of the HPPPA, HAPPA and PNSi.

3.3. Characterisation of treated fabrics

Thermal characteristics of untreated and treated cotton or cotton/polyester fabrics were tested by TGA. Fabrics being heated from room temperature to 600°C under a nitrogen flow with 10°C/min heating rate. Thermal decomposition temperature (onset temperature) and mass loss data are given in Table 1. These data determine the thermal stability of the fabrics and the results are listed in Table 1. TGA thermographs for untreated and treated cotton or cotton/polyester fabrics with PNSi (different concentration) and MgO-NPs (10 g/l) were illustrated in Figure 5.

The figure shows that treated fabrics with PNSi and MgO-NPs decompose in a one stage which occurs from 280 to 400°C as a result of the initiation of the process of breaking up the main cellulosic chain [37]. The pyrolysis of cellulosic chain has the onset temperature which affected by treating the fabrics with any concentration from PNSi/MgONPs composite.

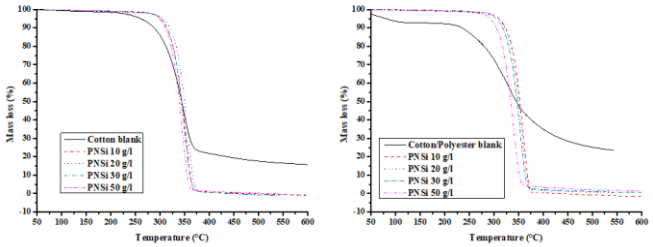

Figure 5. TGA thermograph of both untreated and treated fabrics with PNSi and MgO-NPs.

Table 1. TGA data for both untreated and treated fabrics with PNSi and MgONPs.

PNSi (g/l)	Cotton		Cotton/polyester	
	Mass loss (%)	T onset (°C)	Mass loss (%)	T onset (°C)
0	84.24	310	99.8	278
10	100	330	89.2	332
20	99	326	97.9	332
30	98	323	97.9	333
50	98	323	96.4	335

LOI and vertical tests are broadly used for assessing the flame-retarding efficiency of materials. Generally, it is known that, LOI values is the minimum concentration of oxygen required for the ignition of materials. The vertical test is mostly used to evaluate the ignition and flame spread of materials. Vertical test observed the result is rating between 0 and 5. Rating 0 is highest and 5 is the lowest flame retarding rating. This rating (0) demonstrates that, the fire cannot spread upwards, though the rating 1 and 5 it provides the possibility of non-flaming.

Table 2 displays the LOI values and vertical test rating for untreated and treated both fabrics (cotton and cotton/polyester). The data provide that, once treated fabrics are exposed to fire, a char layer that does not effectively combust will form on the polymer surface. This char layer serves as a powerful shield and protection for the polymer. It can keep the underlying materials from being exposed to oxygen and fire. The structure and producing of this char layer is attributed to the PNSi and MgONPs. Generally, to accomplish a level of fire retardancy, the LOI value must be more than 26 [38, 39]. From Table 2, it is observed that, the LOI values of both treated fabrics increase with an increasing in the PNSi content. Furthermore, all of the treated fabrics show a flame-retarding effects.

Physical and mechanical properties of both untreated and treated fabrics are shown in Table 2. Undeniably, standing out from the untreated one, tensile strength and elongation at a break were decreased. In addition, increasing in roughness value and crease recovery angle (CRA) might be because of the presence of hyperbranched polymer. This increment causes an improve in the fabric properties which is due to that the polymer filled all presence cavities on the fabric surface.

Table 2. Effect of PNSi contents on the nitrogen content and flame retardancy of the treated fabrics.

Fabrics	PNSi	Elemental analysis		Mechanical and physical properties					Fire resistance	
		N %	P %	Tensile Strength (kg)	Elongation at a break (%)	Roughness (µm)	CRA		LOI	Rating (V)
							warp	weft		
Cotton	Blank	0	0	41.8	15.5	17.65	50.3	45.4	18.11	5
	10	6.44	1.97	41.2	15.3	14.14	46.4	42.9	32.23	3
	20	6.61	2.13	40.6	15.4	16.72	45.8	42.1	33.35	2
	30	6.73	2.26	40.5	15.2	16.98	44.2	41.5	35.73	0
	50	6.87	2.34	40.2	15.2	17.43	43.9	41.1	35.96	0
Cotton/Polyester	Blank	0	0	46.6	18.4	19.76	65.7	57.5	13.6	5
	10	6.32	1.56	45.93	18.16	15.83	60.6	54.3	24.20	3
	20	6.49	1.69	45.26	18.28	18.72	59.8	53.3	25.04	2
	30	6.60	1.79	45.15	18.04	19.01	57.7	52.6	26.83	0
	50	6.74	1.85	44.82	18.04	19.51	57.3	52.5	27.00	0

From disc diffusion method, as expected, presence of nitrogen sand silicon centres with MgO-NPs in the composite increase the antibacterial properties. The inhibition zone of treated fabrics was recorded in Table 3. Results in Table 3, untreated cotton or cotton/polyester fabrics show no zone of inhibition, which providing that they doesn't inhibit bacterial activity. All treated fabrics with a prepared composite from 10 to 50 g/l in presence and absence of MgO-NPs led to improve the antibacterial activity.

The mechanism of amino and silicon unit as antibacterial agents was reported before, that is each of them can bound to cell membrane of the bacteria to disturb it and to inhibits their growth due to leakage of intracellular components [40-45].

As reported before, the antibacterial activity of amino groups had more effective bacterial inhibition on *S. aureus* than *E. coli*, because of the different composition of cell walls[46-48]. The *E. coli* (which is a typical Gram-negative bacterium) outer cell wall consist of a thin membrane from peptide polyglycogen and the outer membrane consist of three constituents lipoprotein, lipopolysaccharide and phospholipids. Therefore, the outer membrane has a potential barrier against foreign molecules [47, 49]. In addition, the cell wall of S. aureus bacteria (which is a typical Gram-positive bacterium) is peptide polyglycogen. This layer composed of pores networks, which allow foreign molecules to react with the cell without any difficulty.

Table 3 represents that, treated fabrics (cotton or cotton/polyester) have practically identical antibacterial activity and it has progressively viable inhibition on *S. aureus* than *E. coli.* It was seen from Table 3 that, the presence of MgONPs prompts expanded hindrance reflected by improvement in diameter and in the meantime the composite is progressively successful on both gram (+ve) and Gram (−ve) bacteria due to the nano-structure of MgO-NPs.

Table 3. Antibacterial properties of the treated fabrics.

Sample	PNSI (g/l)	*Staphylococcus aureus (S. aureus)*		*Escherichia coli (E. coli)*	
		Without MgO-NPs	With MgO-NPs (10 g/l)	Without MgO-NPs	With MgO-NPs (10 g/l)
Cotton Fabric 100 %	Blank	0	0	0	0
	10	12.3	14.4	10.5	12.1
	20	15.2	17.8	13	15.0
	30	19.6	22.9	16.7	19.2
	50	23.3	27.3	19.9	22.9
Cotton/Polyester Fabric 100 %	Blank	0	0	0	0
	10	10.1	11.8	8.6	9.8
	20	12.7	14.8	10.8	12.3
	30	15.3	17.9	13.1	14.9
	50	19.2	22.4	16.4	18.7

4. CONCLUSIONS

During this research, Magnesium oxide nanoparticles (MgO-NPs) were synthesised using Licorice root extract and characterized using FT-IR, TEM and XRD. TEM and particle size analysis confirmed that the size of the nanoparticles ranged from 20 to 40 nm. XRD analysis provides that synthesized nanoparticles have a cubic structure. Characterisation of HAPPA and PNSi composite have been provided through NMR and FT-IR measurements which they confirmed the synthesised of both compounds.

Treated fabrics with PNSi and MgO-NPs have been evaluated for the antibacterial properties and confirmed a good antibacterial properties against both gram negative and gram positive bacteria. In addition, mechanical and physical properties provide that, elongation at a break and tensile strength of treated fabrics were decreased, besides that, roughness and crease recovery angle (CRA) values in both warp and weft directions were increased. That was attributed to presence of hyperbranced polymer which filled all the cavities and hols on the surface of the cotton fabric.

Furthermore, flame retardant properties have been investigated using thermal gravimetrical analysis, vertical test and Limiting oxygen index. These test methods provide that, the pyrolysis of cellulosic chain has the onset temperature which affected by treating the fabrics with PNSi/ MgO-NPs concentration composite. LOI values of both treated fabrics increase with an increasing in the PNSi content. Furthermore, all of the treated fabrics provide an excellent flame-retarding effects.

5. REFERENCES

1. Jadhav, S.D. A review of non-halogenated flame retardant. *The Pharma Innovation Journal* **2018**, *7*, 380-386.
2. Levchik, S.V. *Introduction To Flame Retardancy And Polymer Flammability, in Flame Retardant Polymer Nanocomposites*, A.B. Morgan and C.A. Wilkie, John Wiley & Sons, Inc., 2007; https://doi.org/10.1002/9780470109038.ch1.
3. Mohamed, A.L.; Hassabo, A.G. *Flame Retardant of Cellulosic Materials and Their Composites, in Flame Retardants*, Visakh, P.M.; Arao, Y. Springer International Publishing, 2015; pp. 247-314, https://doi.org/10.1007/978-3-319-03467-6_10.
4. Hassabo, A.G.; Mohamed, A.L.; Shaarawy, S.; Hebeish, A. Novel micro-composites based on phosphorylated biopolymer/polyethyleneimine/clay mixture for cotton multi-functionalities performance. *Biosci. Res.* **2018**, *15*, 2568-2582.
5. Ye, L.; Wu, Q.; Qu, B. Synergistic effects of fumed silica on intumescent flame-retardant polypropylene. *J. Appl. Polym. Sci.* **2010**, *115*, 3508-3515, https://doi.org/10.1002/app.30585.
6. Chen, X.L.; Jiao, C.M.; Wang, Y. Synergistic effects of iron powder on intumescent flame retardant polypropylene system. *Express Polym. Lett.* **2009**, *3*, 359-365, http://dx.doi.org/10.3144/expresspolymlett.2009.45
7. Wu, N.; Yang, R. Effects of metal oxides on intumescent flame-retardant polypropylene. *Polym. Adv. Technol*. **2011**, *22*, 495-501, https://doi.org/10.1002/pat.1539.
8. Nie, S.; Hu, Y.; Song, L.; He, S.; Yang, D. Study on a novel and efficient flame retardant synergist–nanoporous nickel phosphates VSB-1 with intumescent flame retardants in polypropylene. *Polym. Adv. Technol*. **2008**, *19*, 489-495, https://doi.org/10.1002/pat.1088.
9. Hebeish, A.; Shaarawy, S.; Hassabo, A.G.; El-Shafei, A. Eco-Friendly Multifinishing of cotton through Inclusion of Motmorillonite/chitosan Hybrid Nanocomposite. *Der Pharma Chemica* **2016**, *8*, 259-271.
10. Liu, Y.; Wang, J.S.; Deng, C.L.; Wang, D.Y.; Song, Y.P.; Wang, Y.Z. The synergistic flame-retardant effect of O-MMT on the intumescent flame-retardant PP/CA/APP systems. *Polymers for Advanced Technologies* **2010**, *21*, 789-796, https://doi.org/10.1002/pat.1502.
11. Ellis, W.D.; Rowel, R.M. Flame-Retardant Treatment Of Wood With A Diisocyanate And An Oligomer Phosphonate. *Wood Fiber Sci*. **1989**, *21*, 367-375.
12. Wang, L.; Yang, R.; Yuan, B.; Liu, Y.; Liu, C. The antiviral and antimicrobial activities of licorice, a widely-used Chinese herb. *Acta Pharmaceutica Sinica B* **2015**, *5*, 310-315, https://dx.doi.org/10.1016%2Fj.apsb.2015.05.005.
13. Zhang, Y.W.; Luo, H.L.; Chang, Y.F.; Jiao, L.J.; Liu, K. Effects of liquorice extract on the activity and gene expression level of antioxidant enzymes in longissimus dorsi muscle of Tan lamb. *Small Ruminant Res* **2017**, *154*, 23-28, https://doi.org/10.1016/j.smallrumres.2017.06.012.
14. Shabkhiz, M.A.; Eikani, M.H.; Bashiri, Z.S.; Golmohammad, F. Superheated water extraction of glycyrrhizic acid from licorice root. *Food Chem* **2016**, *210*, 396-401, https://doi.org/10.1016/j.foodchem.2016.05.006.
15. Li, Y.H.; Li, Y.N.; Li, H.T.; Qi, Y.R.; Wu, Z.F.; Yang, M. Comparative study of microwave-vacuum and vacuum drying on the physicochemical properties and antioxidant capacity of licorice extract powder. Powder Technology 2017, *320*, 540-545, https://doi.org/10.1016/j.powtec.2017.07.076.
16. Rizzato, G.; Scalabrin, E.; Radaelli, M.;Capodaglio, G.; Piccolo, O. A new exploration of licorice metabolome. *Food Chem* **2017**, *221*, 959-968, https://doi.org/10.1016/j.foodchem.2016.11.068.
17. Wang, W.; Qiao, X.; Chen, J.; Li, H. Facile synthesis of magnesium oxide nanoplates via chemical precipitation. *Materials Letters* **2007**, *61*, 3218-3220, https://doi.org/10.1016/j.matlet.2006.11.071.
18. Venkatram, M.; Rao, N.M.H.N.; Gaikwad, A.; Mankunipoyil, S.A.; Ramakrishna, S.; Ratna, P.A. Antibacterial and Flame Retardant Properties of Ag-Mgo/Nylon 6 Electrospun Nanofibers for Protective Applications. Clothing and Textiles Research Journal, **2018**, 36, 296-309
19. Riyadh, S.M.; Khalil, K.D.; Aljuhani, A. Chitosan-MgO Nanocomposite: One Pot Preparation and Its Utility as an Ecofriendly Biocatalyst in the Synthesis of Thiazoles and [1,3,4]thiadiazoles. *Nanomaterials* **2018,** *8*, 928, https://dx.doi.org/10.3390%2Fnano8110928.
20. Deilami, K.; Sayyahi, S. Porous hierarchical magnesium oxide-based heterogeneous catalyst for the Knoevenagel condensation. *Russ. J. Gen. Chem.* **2017**, *87*, 1085-1086, https://doi.org/10.1134/S1070363217050310.
21. Kumar, D.; Reddy, V.B.; Mishra, B.G.; Rana, R.K.; Nadagouda, M.N.; Varma, R.S. Nanosized magnesium oxide as catalyst for the rapid and green synthesis of substituted 2-amino-2-chromenes. *Tetrahedron* **2007**, *63*, 3093-3097, https://doi.org/10.1016/j.tet.2007.02.019.
22. Wang, J.A.; Novaro, O.; Bokhimi, X.; López, T.; Gómez, R.; Navarrete, J.; Llanos, M.E.; López-Salinas, E. Characterisation s of the thermal decomposition of brucite prepared by sol–gel technique for synthesis of nanocrystalline MgO. *Materials Letters* **1998**, *35*, 317-323, https://doi.org/10.1016/S0167-577X(97)00273-5.
23. Jhansi, K.; Jayarambabu, N.; Reddy, K.P.; Reddy, N.M.; Suvarna, R.P.; Rao, K.V.; Kumar, V.R.; Rajendar, V. Biosynthesis of Mgo Nanoparticles Using Mushroom Extract: Effect on Peanut (Arachis Hypogaea L.) Seed Germination. 3 Biotech, **2017**, *7*, 263-263
24. Mohamed, A.L.; Hassabo, A.G.; Shaarawy, S.; Hebeish, A. Benign development of cotton with antibacterial activity and metal sorpability through introduction amino triazole moieties and AgNPs in cotton structure pre-treated with periodate. *Carbohydr. Polym.* **2017**, *178*, 251-259, https://doi.org/10.1016/j.carbpol.2017.09.024.
25. Gowri, S.; Sundrarajan, M.; Selvam, S.; Gandhi, R.R.; Suresh, J. Antibacterial Effect of Nyctanthes arbor-tristis Extract and Biosynthesized TiO_2 Nanoparticles Coated on Cotton Fabric. *Advanced Science, Engineering and Medicine* **2012**, *4*, 55-61, https://doi.org/10.1166/asem.2012.1114.
26. Hassabo, A.G.; Nada, A.A.; Ibrahim, H.M.; Abou-Zeid, N.Y. Impregnation of silver nanoparticles into polysaccharide substrates and their properties. *Carbohydr. Polym*. **2015**, *122*, 343-350, https://doi.org/10.1016/j.carbpol.2014.03.009.

27. Hassabo, A.G.; Salama, M.; Popescu, C. Characterisation s of PVA composites based on recycled ultrafine cotton and wool powders. *Res. Rev. BioSci*. **2015**, *10*, 147-158.
28. ASTM Standard Test Method (ASTM D 2863–17), *Standard Test Method for Measuring the Minimum Oxygen Concentration to Support Candle-Like Combustion of Plastics (Oxygen Index)*, ASTM International: West Conshohocken, PA. 2018.
29. AATCC Test Method (34-1969), *Vertical Burning Test Method in Fire Resistance of Textile Fabrics*, Technical Manual Method of the American Association of Textile Chemists and Colorists: USA. 1972; pp. 201–202.
30. ASTM Standard Test Method (ASTM D 1683/D 1683M − 17), *Standard Test Method for Failure in Sewn Seams of Woven Fabrics*, ASTM International: West Conshohocken, PA. 2011.
31. ASTM Standard Test Method (ASTM D1388 − 14e1), *Standard Test Methods for Stiffness of Fabrics*, ASTM International: West Conshohocken, PA. 2016.
32. Soumitra, K.; Subhadra, C. Synthesis and Characterisation of one-dimensional MgO nanostructures. *J Nanosci Nanotechnol* **2006**, *6*, 1447-1452, http://dx.doi.org/10.1166/jnn.2006.307.
33. Wu, J.; Yan, H.; Zhang, X.; Wei, L.; Liu, X.; Xu, B. Magnesium hydroxide nanoparticles synthesized in water-in-oil microemulsions. *J. Colloid Interface Sci.* **2008**, *324*, 167-171, https://doi.org/10.1016/j.jcis.2008.03.052.
34. Tian, Y.; Wang, G.; Li, F.; Evans, D.G. Synthesis and thermo-optical stability of o-methyl red-intercalated Ni–Fe layered double hydroxide material. *Materials Letters* **2007**, *61*, 1662-1666, https://doi.org/10.1016/j.matlet.2006.07.094.
35. Çelebi, F.; Polat, O.; Aras, L.; Gündüz, G.; Akhmedov, I.M.; Synthesis and Characterisation of water-dispersed flame-retardant polyurethane resin using phosphorus-containing chain extender. *J. Appl. Polym. Sci.* **2004**, *91*, 1314-1321, https://doi.org/10.1002/app.13279.
36. Chiu, S.H.; Wu, C.L.; Lee, H.T.; Gu, J.H.; Suen, M.C. Synthesis and characterisation of novel flame retardant polyurethanes containing designed phosphorus units. *J. Polym. Res.* **2016**, *23*, https://doi.org/10.1007/s10965-016-1098-y.
37. Dutikova, O.S.; Strekalova, Y.V.; Zubkova, N.S.; Butylkina, N.G.; Konstantinova, N.I.; Naganovskii, Y.K. Characteristics of thermooxidative decomposition of cotton and polyester blends. *Fibre Chemistry* **2004**, *36*, 370-373, http://dx.doi.org/10.1007/s10692-005-0011-y.
38. Cullis, C.F.; Hirschler, M.M. Char formation from Polyolefins. *Europian Polym Journal* **1984**, *20*, 53-60, https://doi.org/10.1016/0014-3057(84)90222-2.
39. Wang, D.Y.; Liu, Y.; Wang, Y.Z.; Artiles, C.P.; Hull, T.R.; Price, D. Fire retardancy of a reactively extruded intumescent flame retardant polyethylene system enhanced by metal chelates. *Polym. Degrad. Stab.* **2007**, *92*, 1592-1598, https://doi.org/10.1016/j.polymdegradstab.2007.04.015.
40. Papineau, A.M.; Hoover, D.G.; Knorr, D.; Farkas, D.F. Antimicrobial effect of water-soluble chitosans with high hydrostatic pressure. *Food Biotechnology* **1991**, *5*, 45-57, https://doi.org/10.1080/08905439109549790.
41. Ibrahim, N.A.; Nada, A.A.; Eid, B.M.; Al-Moghazy, M.; Hassabo, A.G.; Abou-Zeid, N.Y. Nano-structured metal oxides: synthesis, Characterisation and application for multifunctional cotton fabric. *Advances in Natural Sciences: Nanoscience and Nanotechnology* **2018**, *9*, 35014, https://doi.org/10.1088/2043-6254/aadc2c.
42. Abou-Zeid, N.Y.; Waly, A.I.; Kandile, N.G.; Rushdy, A.A.; El-Sheikh, M.A.; Ibrahim, H.M.; Preparation, Characterisation and Antibacterial Properties of Cyanoethylchitosan and Cellulose Acetate Polymer Blended Films. *Carbohydr. Polym.* **2011**, *84*, 223-230, https://doi.org/10.1016/j.carbpol.2010.11.026
43. Mohamed, A.L.; Hassabo, A.G.; Nada, A.A.; Abou-Zeid, N.Y. Properties of Cellulosic Fabrics Treated by Water-repellent Emulsions. *Indian J. Fibre Text. Res*. **2017**, *42*, 223-229.
44. Waly, A.I.; Abou-Zeid, N.Y.; Marie, M.M.; El-Sheikh, M.A.; Mohamed, A.L. Special Finishing of Cotton to Impart Flame-Retardancy, Easy Care Finishing and Antimicrobial Properties. *RJTA* **2009**, *13*, 10-26, https://doi.org/10.1108/RJTA-13-03-2009-B002.
45. Sudarshan, N.R.; Hoover, D.G.; Knorr, D. Antibacterial action of chitosan. *Food Biotechnology* **1992**, *6*, 257-272, https://doi.org/10.1080/08905439209549838.
46. Chung, Y.C.; Su, Y.P.; Chen, C.C.; Jia, G.; Wang, H.L.; Wu, J.C.; Lin, J.G. Relationship between antibacterial activity of chitosan and surface characteristics of cell wall. *Acta Pharmacol Sin* **2004**, *25*, 932-6.
47. Sun, L.; Du, Y.; Fan, L.; Chen, X.; Yang, J. Preparation, Characterisation and antimicrobial activity of quaternized carboxymethyl chitosan and application as pulp-cap. *Polymer* **2006**, *47*, 1796-1804, https://doi.org/10.1016/j.polymer.2006.01.073.
48. Xu, T.; Xin, M.; Li, M.; Huang, H.; Zhou, S.; Liu, J. Synthesis, Characterisation , and antibacterial activity of N,O-quaternary ammonium chitosan. *Carbohydr. Res*. **2011**, *346*, 2445-50, https://doi.org/10.1016/j.carres.2011.08.002.
49. Kong, M.; Chen, X.G.; Liu, C.S.; Liu, C.G.; Meng, X.H.; Le, J.Y. Antibacterial mechanism of chitosan microspheres in a solid dispersing system against E. coli. *Colloids Surfaces B: Biointerfaces* **2008**, *65* 197-202, https://doi.org/10.1016/j.colsurfb.2008.04.003.

6. ACKNOWLEDGEMENTS

The authors also gratefully grateful acknowledge to National Research Centre (NRC) for facilities provided.